Influence of length on shock-induced breaking behavior of copper nanowires

Yunhong Liu, Jianwei Zhao,* and Fenying Wang
Key Laboratory of Analytical Chemistry for Life Science (Ministry of Education), School of Chemistry and Chemical Engineering, Nanjing University, Nanjing 210008, China

(Received 7 May 2009; revised manuscript received 16 July 2009; published 17 September 2009)

In this study, molecular-dynamics simulations were employed with an embedded-atom method to investigate the shock-induced breaking behavior of single-crystal copper nanowires along a [100] direction at a constant strain rate. The cross section was fixed at 1.8 nm^2 for all model nanowires. The results showed that the final breaking position depended on the nanowire length. When it was less than 6.0 nm, the most probable breaking position was located at the center of the nanowires. However, it gradually shifted to the ends as the nanowire length increased over 6.0 nm. The longitudinal wave theory was used to interpret the shift of the most probable breaking position.

DOI: 10.1103/PhysRevB.80.115417 PACS number(s): 61.46.−w, 62.25.−g, 62.20.−x, 62.23.Hj

In the past decade, metal nanowires have been the focus of intense research due to their mechanical, thermal, and electrical properties. With the multifunctional properties of the nanowire, it is extremely important for the emerging applications such as active components of circuits,[1] sensors,[2,3] and actuators in nanoelectromechanical systems.[4] Well understanding of the properties and the behaviors of the metallic nanowires is critical to the success of the design, manufacture, and manipulation of nanodevices.

Molecular-dynamics (MD) simulation as an effective method is employed to study the mechanical properties and the breaking behaviors of nanowires. Wu *et al.*[5] and Park *et al.*[6] studied the nanowire failure by performing MD simulations. Kang *et al.*[7] investigated the mechanical deformation of copper nanowires under elongation, shearing, rotation, and rotated elongation. Importantly, many studies have demonstrated that the mechanical properties strongly depend on the nanowire dimensions.[8,9] Hasmy[10] demonstrated that the 5*d* metals experienced a reorientation from {100} to {111} orientation if the film thickness is less than a critical thickness. However, most of these theoretical simulations focused on the infinite long nanowires with a periodicity along the wire axis, and the dynamic behavior of nanowires by using the free boundary condition was reported rarely. Since the Rayleigh instability[11] is remarkable for the nanowires with large length-to-diameter ratio, especially at high strain rates, the study on the length influence is of great significance in the fundamental research and possible applications.

From the previous studies,[12] we found that the final breaking positions followed a statistical distribution with a most probable breaking position (MPBP). Moreover, the breaking behavior and breaking position showed a strain-rate dependence. When the strain rate was up to the shock range of above 1.0% ps^{-1}, partial or whole structural amorphization was observed.[12–17] Shock wave theory has been used for decades to interpret the behavior of materials under extreme conditions.[18–20] Most experimental studies[18–20] of shock wave in metals were carried out by polycrystalline samples. To date, it is difficult to give a direct measurement of the dynamic deformation process during high-strain rates loading at nanoscale. Molecular-dynamics simulations can provide detailed structure of the atomistic evolution of the shocked materials. For example, the deformation behavior of the shocked single crystal showed clear orientation dependence.[21–23] These investigations can provide a guide to the experimental efforts. Although significant progress has been made to understand the nanowire properties, some points are still unclear. Especially the physical basis that dominates the shift of MPBP is not yet achieved.

In the present work, the mechanical properties of copper nanowires with length-to-diameter ratio from 1.2 to 6.0 at a constant strain rate have been systematically studied. The length influence on the shift of MPBP has been interpreted by a shock wave propagation mechanism.[21–24]

Molecular-dynamics simulations were performed on the solid copper nanowires using embedded-atom method (EAM),[25,26] which could provide a relevant description of the transition metals of either a face-centered cubic or body-centered cubic structure. Among the various types of *n*-body potentials, the EAM potential is one of the most realistic and promising potentials. The Verlet leapfrog algorithm[27] was used for the integration of motion equations to obtain velocity and trajectories of atoms, with the time step of 1.6 fs. Nosé-Hoover thermostat[28,29] was applied so as to keep the system temperature constantly at 300 K. The simulations were performed with self-developed software, NANOMD.[30] The reliability of the software as well as the algorithms has been validated not only by a large amount of theoretical simulations,[12,31] but also with the comparison to the experimental measurements.[32]

In this study, the initial geometric configurations of nanowires were generated from a rectangular lattice along the [100] crystallographic direction. The cross section was square with a side of five crystal cells. In order to investigate the length effect, the nanowire length was varied from six to 30 crystal cells (2.2 to 10.9 nm). Different but enough relaxation time was allowed to obtain different stable initial states. 300 samples were studied for each length. More than 6,600 samples were employed totally. Starting from the equilibrium configuration, uniaxial tensile was conducted along the *z* direction at constant strain rate of 3.1% ps^{-1} by moving the fixed atomic layers placed at the ends of the nanowire as shown in Fig. 1.

Average stresses along *z* direction of all the atoms were recorded every step by virial scheme.[33] The final breaking positions evaluated as ANR=atom number in the smaller

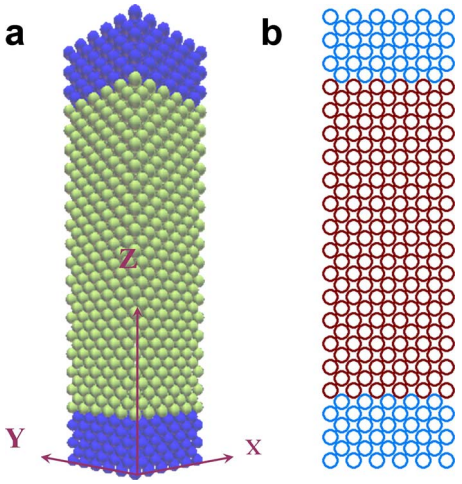

FIG. 1. (Color online) Single-crystalline copper nanowires positioned with [100] surfaces out. The wire's sizes is $5a \times 5a \times La$ (where a is copper's lattice constant 0.362 nm, and L vary from 6 to 30.) The two ends with three lattices thick are free during relaxation but fixed in x-y plane when the uniaxial strain is performed at constant speed 3.1% ps^{-1}.

part after breaking/total atom number of the nanowire $\times 100\%$.[12]

The mechanical properties of the nanowires as a function of system size, including stress-strain relationship, yield strain, and average Young's modulus, are shown in Fig. 2. Figure 2(a) shows the typical stress-strain responses of copper nanowires with different length from 2.2 to 10.9 nm at a constant temperature of 300 K. Strain is defined as a dimensionless quality, $\varepsilon=(l-l_0)/l_0$, where l is the current wire length and l_0 is the length just after the preliminary relaxation. The stress increases with increasing strain at the first linear stage. After the yield point, corresponding to 0.1 yield strain and ~9.0 GPa yield stress, stress drops rapidly for most nanowires, indicating that the nanowires experience an abrupt dislocation caused by the mechanical stretch. However, for some cases, taking the system of 3.6 nm for example, stress declines after the yield point, but rises again to about 8.0 GPa. This recovery of stress is, probably, caused by the crystal reorientation.[34] With the increase in strain, the stress displays slight fluctuations, implying that the nanowire experiences recrystallization into a temporary stable structure. These processes repeat themselves continuously until the final breaking. The stress-strain responses are sensitive to the system size, and the fluctuation exhibits the size dependence as well. Figure 2(b) gives the mean-square error of the stress, showing a rapid drop at the fist stage and a stable value for those long nanowires.

The statistical analysis of yield strain obtained from 300 samples for each cross section accords with a Gaussian-type distribution [insert in Fig. 2(c)]. In spite of the big variation for short wires, the mean yield strain decreases almost exponentially from 0.14 to 0.10 with the length increasing. The data error of yield strain is presented in Fig. 2(d), which decreases as the nanowire length increases. It illustrates again that the stochastic motion of atoms becomes minor as the system size increases.

Young's modulus, as an effective approach to evaluate the mechanical strength of the nanowire, is adopted with the force approach.[35] Before the yield point, the stress increases linearly with the increasing strain. Young's modulus can be

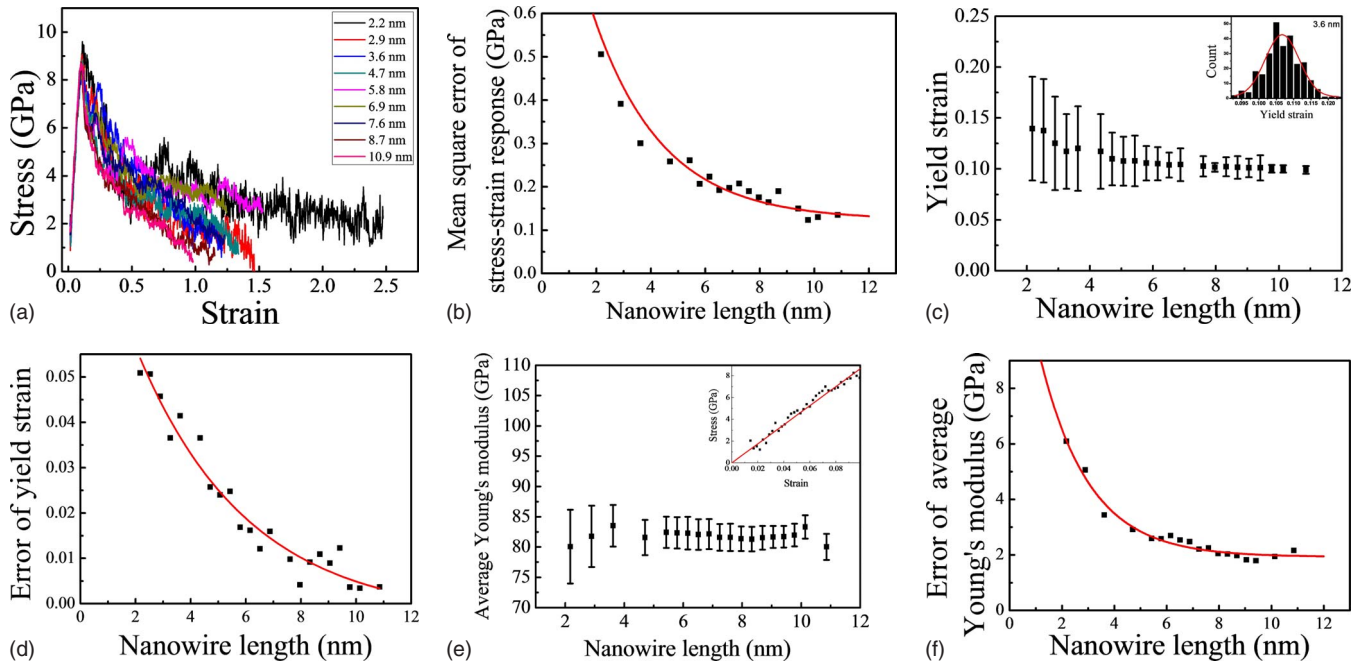

FIG. 2. (Color online) (a) Typical strain-stress responses of the nanowires with different crystal lattices from 6 to 30 corresponding length from 2.2 to 10.9 nm at $T=300$ K and $\varepsilon=3.1\%$ ps^{-1}. (b) The degree of the fluctuation of stress-strain response. We get the mean-square error of the margin of initial stress-strain response and the interpolated curve. (c) The average Young's modulus corresponding to 300 samples for each nanowire length from 2.2 to 10.9 nm. (d) The error of the average yield strain. (e) Average yield strain for different length of nanowire. (f) The error of the average Young's modulus.

obtained through the linear fitting. The inserted figure of Fig. 2(e) displays a typical stress-strain curve in the linear stage of the 2.9 nm sample. In spite of some fluctuations caused by the atomic motion, the correlation coefficient of the linear fitting is as high as 0.99. The averaged Young's modulus is averaged from 300 samples for each length. It varies a little from 80.1 ± 6.1 to 83.5 ± 1.9 GPa in a wide range of nanowire length. Figure 2(f) exhibits the error of average Young's modulus as a function of the nanowire length. Similar to other properties, the error of Young's modulus also decreases rapidly and, then, reaches a plateau.

From the results above, we find that the average error for most properties shows a strong size-dependence. We would like to briefly comment on this point. As presented in Figs. 2(b), 2(d), and 2(f), all the statistical errors decrease with the nanowire length increasing. This indicates that when the nanowire size is small enough, the indeterminacy caused by stochastic motion of atoms is remarkable just as the microscopic particles. On the other hand, the determinacy increases with increasing the nanowire length. This also infers that the macroscopic understanding might be valid for the nanowires with longer dimension, though the statistic fluctuation becomes acute as size reduced.

Materials failure is of profound importance for the utility in devices. If the breaking position is predictable, the nanowire can be strengthened near the breaking position to avoid failure. Although the single breaking case is not predictable, many breaking cases show a statistic feature. Figure 3(a) presents the representative snapshots of copper nanowires with different length from 2.2 to 10.9 nm at the breaking moment. In most cases, the final breaking position occurs at the central part of the nanowire when it is short. As the nanowire length increases, the breaking position gradually shifts to the ends. Figure 3(b) gives the statistical histograms fitted with Gaussian function over 300 samples for each length. The peak of the curve is related to the most probable breaking position abbreviated as MPBP. When the nanowire length is smaller than 4.7 nm, MPBP is around 50%, indicating a symmetrical breaking of the nanowire. When the nanowire length increases, the MPBP shifts from the nanowire center to the ends. For example, the 5.8 nm sample has two ANR values of 35% and 65%, respectively.

Here we would like to address another important question: what is the most crucial factor dominating the shift of MPBP? Answering this question will be helpful to the design, manufacture, and manipulation of nanodevices. In order to give insight into the physical basis of the MPBP shift, we analyze the nanowire deformation from the microscopic viewpoint and attempt to combine strain-wave propagation theory to interpret the observation.

When the nanowires undergo a high-rate stretching, the loading of mechanical stress vibrates the atoms within a certain extent, resulting in an alternate distribution of atomic density. The atoms in the lower atomic density regions have higher cohesive force, whereas higher repulsive force is in the higher atomic density region. The transient inhomogeneity of atomic density distribution may propagate along the nanowire uniaxial axis, just like the wave propagation.

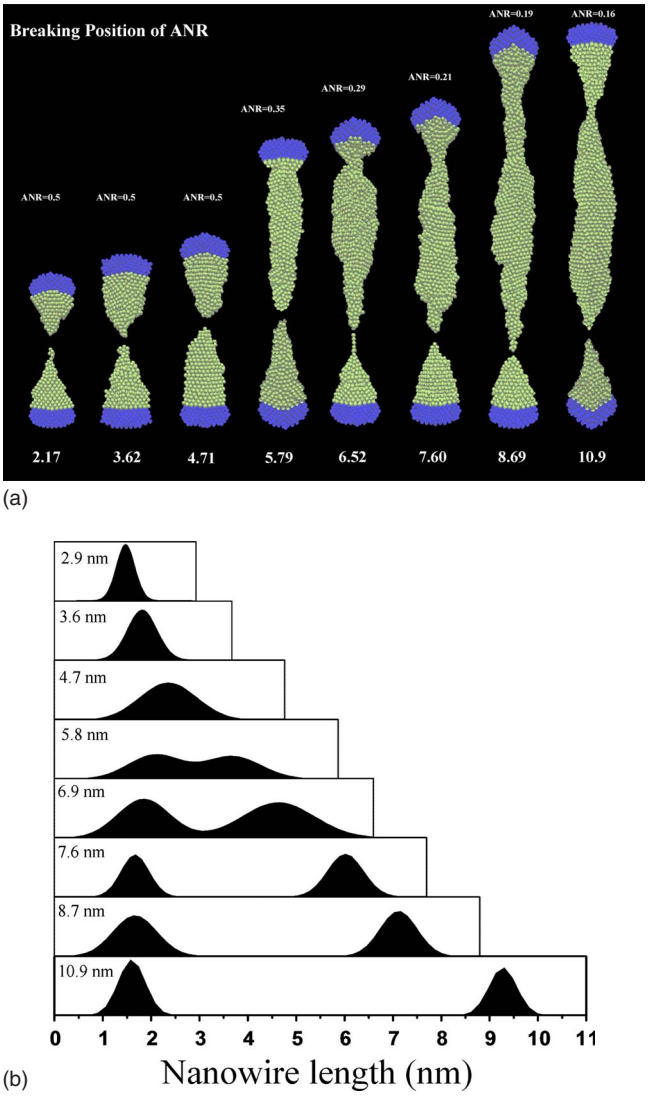

FIG. 3. (Color online) (a) The snapshots of copper nanowire with the length from 2.2 to 10.9 nm at the breaking moment. (b) The distribution of breaking position along [100] direction with different nanowire length from 2.9 to 10.9 nm.

Therefore, shock wave propagation theory, which is applicable in many macroscopic systems, might be attempted to interpret these observations. Holid *et al.*,[36,37] Kadau *et al.*,[38] and Bringa *et al.*[39] studied the shock wave propagation in solid. They demonstrated the existence of shock wave in nanoscale. This concept should benefit the understanding of MPBP shift.

When the nanowire is subjected to a strain rate above the amorphization limit, unidirectional and longitudinal strain-wave propagations are dominant in the homogeneous medium. The shock waves propagate repeatedly through the whole nanowire, and then overlap in a certain position. The concentrated wave energy is, then, converted to the kinetic energy of atoms. In most cases, the metal atoms are restricted in a tiny scope, vibrating around their equilibrated position. When the atoms are activated by the consistent shock waves, they may have enough energy to break the control of the surrounding bond force. As a result, clear stress drops at

TABLE I. The typical results of different system including the time required to attain atomic break, the approximated strain-wave propagation speed, and the calculated final breaking position. When the nanowire length is small, strain wave annihilated upon hitting the opposite end of the nanowire before attaining the initial atom break, so the time required to attain the atomic break was estimated the second strain wave.

System size (unit: cell 0.362 nm)	U_S approximate the strain-wave propagation speed (nm/ps)	t time required to attain the initial atomic break (ps)	CBP $0.5Us \times t/l$
$5\times5\times6$	3.00	4.50	0.37
$5\times5\times8$	3.03	4.03	0.37
$5\times5\times10$	3.06	3.87	0.43
$5\times5\times13$	3.03	3.54	0.35
$5\times5\times16$	3.04	3.40	0.60
$5\times5\times18$	3.04	3.35	0.71
$5\times5\times22$	3.02	3.27	0.87
$5\times5\times24$	3.03	3.27	0.92

strain of about 0.1 can be observed from the stress-strain curves [Fig. 2(a)]. Near the initial bond breaking position, the breaking behavior occurs continually until a clear neck appears. Around the neck location [Fig. 3(a)], a highly localized amorphous region emerges within the nanowire. The atoms positioning this region are pulled out from their matrix, resulting in the elongation of the nanowire. This process repeats continuously until the nanowire breaks. From this discussion, we can propose that the final breaking position is the consequence of the evolution of the initial breaking position, which is determined by the highest shock wave energy crest, i.e., the central part of the energy crest. The energy crest is determined by the product of the propagation speed, U_S, and the time, t, required to attain the atomic break.

In this paper, the estimated speed of the shock wave propagation U_S is given in a simplified form as the equation $Us=\sqrt{E/\rho}$,[16,40] in which E is the Young's modulus and ρ is the average density of copper, which is estimated to be $8,900\ \mathrm{kg/m^3}$. The time required to attain the initial atomic break corresponds to the yield strain which is shown in Fig. 2(c). So we can obtain the wave propagation distance $d=U_S\times t$. The time (t) required to attain atomic break, the approximated strain-wave propagation speed (U_S), and the calculated final breaking position for different system are summarized in Table I. Figure 4 compares the statistical results from the MD simulations and the calculated results from shock wave propagation theory. When the nanowire length is lager than 4.7 nm, as shown in the right region, the trend of calculated breaking position is in agreement with the statistical results. However, as the nanowire is shorter than 4.7 nm, the calculated breaking position is deviated from the nanowire center that is not in accordance with the simulation results. It is attributed to the effect of the terminal fixed layers. Although the wave propagation theory is instructive for understanding the nanobreaking, other effects, such as surface orientation, cross-section size, interface, and strain rate, should be also involved.[11]

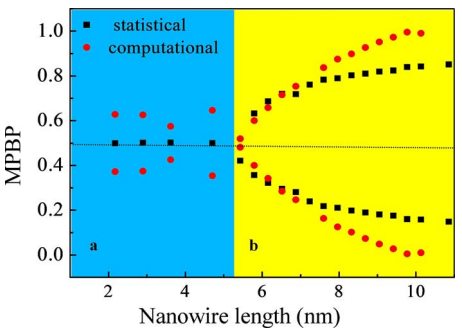

FIG. 4. (Color online) The comparison of the statistical and calculated most breaking position.

In conclusion, we have studied the length influence on the copper nanowire breaking behavior under high-strain-rate stretching by performing molecular-dynamics simulations. The final breaking position exhibits a distribution and the most probable breaking position presents a gradual shift from the center to the ends as the nanowire length increases. Strain-wave propagation theory has been used to explain the shift of most probable breaking position. The simulation results would be helpful to avoid the materials failure by predicting the breaking position.

The shocked behaviors of nanowires could be studied through experimental investigations such as nanowire growth using a laser-induced shock.[24] It should also be noted that we focus only on the influence of length on the breaking behaviors; other controllable variables such as the nanowires cross section, the temperature, and the crystalline orientation have been kept constant in this study. The shock-induced breaking behavior would be different if the simulation conditions are changed. Further study on the influence of temperature and cross section is in process.

This project was supported by the National Natural Science Foundation of China (Grants No. 20873063 and No. 20821063) and National Basic Research Program of China (973 Program, Grant No. 2007CB936302). Moreover, the present work was in part financed by State Key Laboratory of Physical Chemistry of Solid Surfaces (Xiamen University).

*Corresponding author. FAX: +86-25-83596523; zhaojw@nju.edu.cn

[1] N. A. Melosh, A. Boukai, F. Diana, B. Gerardot, A. Badolato, P. M. Petroff, and J. R. Heath, Science **300**, 112 (2003).
[2] Q. Wan, Q. H. Li, Y. J. Chen, T. H. Wang, X. L. He, J. P. Li, and C. L. Lin, Appl. Phys. Lett. **84**, 3654 (2004).
[3] H. Q. Liu, J. Kameoka, D. A. Czaplewski, and H. G. Craighead, Nano Lett. **4**, 671 (2004).
[4] S. Büttgenbach, S. Butefisch, M. Leester-Schadel, and A. Wogersien, Microsyst. Technol. **7**, 165 (2001).
[5] H. A. Wu, A. K. Soh, X. X. Wang and Z. H. Sun, Adv. Fract. Failure Prev. **261-263**, 33 (2004).
[6] H. S. Park and J. A. Zimmerman, Phys. Rev. B **72**, 054106 (2005).
[7] P. Walsh, W. Li, R. K. Kalia, A. Nakano, P. Vashishta, and S. Saini, Appl. Phys. Lett. **78**, 3328 (2001).
[8] B. D. Hall, M. Flüeli, R. Monot, and J. P. Borel, Phys. Rev. B **43**, 3906 (1991).
[9] Y. Kondo and K. Takayanagi, Science **289**, 606 (2000).
[10] A. Hasmy and E. Medina, Phys. Rev. Lett. **88**, 096103 (2002).
[11] F. Kassubek, C. A. Stafford, H. Grabert, and R. E. Goldstein, Nonlinearity **14**, 167 (2001).
[12] D. Wang, J. Zhao, S. Hu, X. Yin, S. Liang, Y. Liu, and S. Deng, Nano Lett. **7**, 1208 (2007).
[13] Y.-H. Wen, Z.-Z. Zhu, and R.-Z. Zhu, Comput. Mater. Sci. **41**, 553 (2008).
[14] P. S. Branício and J. P. Rino, Phys. Rev. B **62**, 16950 (2000).
[15] H. Ikeda, Y. Qi, T. Çagin, K. Samwer, W. L. Johnson, and W. A. Goddard, Phys. Rev. Lett. **82**, 2900 (1999).
[16] A. S. J. Koh and H. P. Lee, Nano Lett. **6**, 2260 (2006).
[17] S. J. A. Koh, H. P. Lee, C. Lu, and Q. H. Cheng, Phys. Rev. B **72**, 085414 (2005).
[18] W. J. Nellis, J. A. Moriarty, A. C. Mitchell, M. Ross, R. G. Dandrea, N. W. Ashcroft, N. C. Holmes, and G. R. Gathers, Phys. Rev. Lett. **60**, 1414 (1988).
[19] W. J. Nellis, A. C. Mitchell, and D. A. Young, J. Appl. Phys. **93**, 304 (2003).
[20] A. C. Mitchell, W. J. Nellis, J. A. Moriarty, R. A. Heinle, N. C. Holmes, R. E. Tipton, and G. W. Repp, J. Appl. Phys. **69**, 2981 (1991).
[21] V. V. Zhakhovskiĭ, S. V. Zybin, K. Nishihara, and S. I. Anisimov, Phys. Rev. Lett. **83**, 1175 (1999).
[22] J. B. Maillet, M. Mareschal, L. Soulard, R. Ravelo, P. S. Lomdahl, T. C. Germann, and B. L. Holian, Phys. Rev. E **63**, 016121 (2000).
[23] B. L. Holian and P. S. Lomdahl, Science **280**, 2085 (1998).
[24] E. M. Bringa, J. U. Cazamias, P. Erhart, J. Stolken, N. Tanushev, B. D. Wirth, R. E. Rudd, and M. J. Caturla, J. Appl. Phys. **96**, 3793 (2004).
[25] R. A. Johnson, Phys. Rev. B **39**, 12554 (1989).
[26] R. A. Johnson, Phys. Rev. B **37**, 3924 (1988).
[27] L. Verlet, Phys. Rev. **159**, 98 (1967).
[28] S. Nosé, J. Chem. Phys. **81**, 511 (1984).
[29] W. G. Hoover, Phys. Rev. A **31**, 1695 (1985).
[30] J. W. Zhao, X. Yin, S. Liang, Y. H. Liu, D. X. Wang, S. Y. Deng, and J. Hou, Chem. Res. Chin. Univ. **24**, 367 (2008).
[31] Y. Liu, F. Wang, J. Zhao, L. Jiang, M. Kiguchi, and K. Murakoshi, Phys. Chem. Chem. Phys. **11**, 6514 (2009).
[32] J. Zhao, K. Murakoshi, X. Yin, M. Kiguchi, Y. Guo, Nan Wang, S. Liang and H. Liu, J. Phys. Chem. C **112**, 20088 (2008).
[33] H. A. Wu, Eur. J. Mech. A/Solids **25**, 370 (2006).
[34] W. Liang, M. Zhou, and F. Ke, Nano Lett. **5**, 2039 (2005).
[35] H. Rafii-Tabar, Phys. Rep. **390**, 235 (2004).
[36] B. L. Holian and G. K. Straub, Phys. Rev. Lett. **43**, 1598 (1979).
[37] B. L. Holian, Phys. Rev. A **37**, 2562 (1988).
[38] K. Kadau, T. C. Germann, P. S. Lomdahl, and B. L. Holian, Science **296**, 1681 (2002).
[39] E. M. Bringa, A. Caro, Y. Wang, M. Victoria, J. M. McNaney, B. A. Remington, R. F. Smith, B. R. Torralva, and H. Van Swygenhoven, Science **309**, 1838 (2005).
[40] M. F. Horstemeyer, M. I. Baskes, and S. J. Plimpton, Acta Mater. **49**, 4363 (2001).